



University  
of Glasgow

Lin, X., Zhou, Z. , Zhang, L. , Tukmanov, A., Abbasi, Q. and Imran, M. A. (2024) RIS-assisted Resource Allocation under Base Stations' Non-cooperation Scheme. In: 2023 IEEE Global Communications Conference: Mobile and Wireless Networks (Globecom 2023), Kuala Lumpur, Malaysia, 4-8 Dec 2023, pp. 7237-7242. ISBN 9798350310900 (doi: [10.1109/GLOBECOM54140.2023.10437328](https://doi.org/10.1109/GLOBECOM54140.2023.10437328))

This is the author version of the work. There may be differences between this version and the published version. You are advised to consult the published version if you wish to cite from it:

<https://doi.org/10.1109/GLOBECOM54140.2023.10437328>

<https://eprints.gla.ac.uk/306374/>

Deposited on: 12 September 2023

Enlighten – Research publications by members of the University of Glasgow  
<https://eprints.gla.ac.uk>

# RIS-assisted Resource Allocation under Base Stations' Non-cooperation Scheme

Xinyi Lin\*, Ziyi Zhou\*, Lei Zhang\*, Anvar Tukmanov<sup>†</sup>, Qammer Abbasi\*, and Muhammad Ali Imran\*

\*School of Engineering, University of Glasgow, G12 8QQ, U.K.

<sup>†</sup>British Telecommunications PLC, Adastral Park, Ipswich, IP5 3RE, U.K.

Email: {x.lin.1, z.zhou.3}@research.gla.ac.uk, {Lei.Zhang, Qammer.Abbasi, Muhammad.Imran}@glasgow.ac.uk, anvar.tukmanov@bt.com

**Abstract**—In this paper, we focus on reconfigurable intelligent surface (RIS)-aided resource allocation under base stations (BSs)' non-cooperation scheme, where the RIS is solely controlled by one BS and should not affect the communication of the adjacent BS. The minimum quality-of-service (QoS) of users served by the RIS-aided BS, minimum effects on the channel quality of the adjacent BS, the sub-channel assignment rule, and the total transmit power constraint are taken into account. Based on these constraints, the sum-rate of users served by the RIS-aided BS is maximized by jointly optimizing the RIS passive beamforming, power allocation, and sub-channel assignment. To tackle the non-convex problem, an efficient algorithm exploiting the techniques of block coordinate descent (BCD) is developed. A two-sided matching (TSM) algorithm is firstly applied to solve the discrete sub-channel assignment optimization. Then the power allocation and RIS passive beamforming are optimized iteratively. To address the non-convexity in optimizing the power allocation and RIS beamforming, a successive convex upper bound approximation method and a multi-ratio fractional programming (FP) with Taylor series approximation-based successive cancellation algorithm (SCA) are used, respectively. The convergence of simulation results proves the validity of our proposed algorithm, and the effects of the numbers of RIS elements and the total transmit power are studied.

**Index Terms**—Reconfigurable intelligent surface, sum-rate maximization, power allocation, sub-channel assignment.

## I. INTRODUCTION

Reconfigurable intelligent surface (RIS) has been recently proposed as a revolutionary technology to enable a controllable wireless propagation environment [1]. Specifically, a RIS is an artificial planar structure consisting of numerous conducting unit cells [2]. By dynamically controlling the unit cell's reflection coefficients, the impinging electromagnetic (EM) signals can be tuned to satisfy any desired characteristics, including directions, gains, etc. This innovative technology is attracting the interests of both academia and industry for its significant contribution to communication performance improvement. Additionally, due to RIS's passive property, the power consumption is very low. Therefore, RISs are suitable to be densely deployed in wireless networks.

RIS-assisted wireless communication has been widely investigated in different scenarios. For example, the authors in [3] studied the security performance in RIS-aided massive multiple-input multiple-output (MIMO) communication systems. Moreover, a RIS-aided uplink multi-antenna non-orthogonal multiple access (NOMA) system was investigated

in [4]. The combination of RIS and NOMA technology was proven to boost both spectrum and energy efficiency. In addition to these works, some efforts have been devoted to RIS-assisted wireless communication systems under more realistic assumptions. Particularly, a multi-user and multi-order-reflection (MUMOR) RIS network was proposed and analyzed in [5], while the MOR signal between reflectors is usually overlooked by most literature. In [6], the effective rate in RIS-aided networks was investigated by considering the phase estimation errors and location uncertainty.

Recently, a few studies have been done on resource allocation in RIS-aided systems for its importance in the practical deployment. Specifically, the authors of [7] studied resource allocation in the RIS-aided downlink NOMA system. To maximize the system throughput, a joint optimization problem over the channel assignment, decoding order, power allocation, and reflection coefficients was formulated. However, the decoding order may not be known to the users, which makes the decoding process challenging. Moreover, this work only considered the single-cell scenario, while the resource allocation in multi-cell networks is more intricate but crucial. A more general RIS-assisted multi-cell mmWave downlink communication network was studied in [8]. A sum-rate maximization problem was proposed by jointly optimizing the RIS beamforming and user association. Nevertheless, the assumption they made that all base stations (BSs) work under the same frequency is impractical. The authors of [9] investigated power allocation and user association in the RIS-assisted multi-cell system. Orthogonal frequencies are allocated to adjacent BSs. Noting that the user association is not realistic, as BSs from different operators do not allow the connection switching. Furthermore, BSs from multiple operators may not make an agreement on cooperatively using RISs due to cost and secure concerns. To the author's best knowledge, no literature considered the scenario where BSs are from different operators, which is defined as BSs' non-cooperation scheme. However, it is crucial to investigate the non-cooperation scheme in RIS-aided systems, as BSs from different operators may not agree to jointly use the RIS or been affected by the unknown RIS. Under BSs' non-cooperation scheme, the conventional resource allocation approaches are not further applicable.

Motivated by these facts, we study the resource allocation under multi-cell BSs' non-cooperation scheme in a RIS-aided

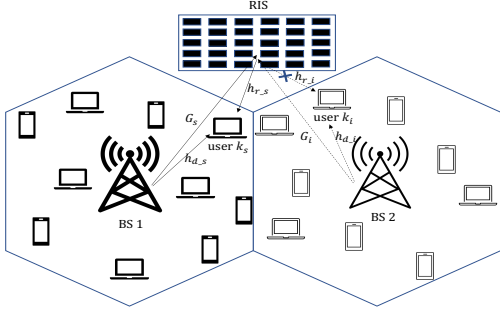


Fig. 1. System model of BSs' non-cooperation scheme.

downlink communication system in this paper. Specifically, we consider a particular non-cooperation scheme that a RIS is solely controlled by one BS, while there is another BS working under an orthogonal frequency band in the adjacent cell that do not need the RIS. On one side, the sub-channel assignment and power allocation are studied as they are important metrics in resource allocation. On the other side, the RIS is designed to further enhance the performance of users served by the dedicated BS (named SUs) while alleviating its effect on the links between the adjacent BS and its serving users (named IUs). Considering the impact of RIS on channels that aim to be either enhanced or unaffected, a sum-rate maximization problem is formulated by jointly optimizing the passive RIS beamforming, sub-channel assignment, and power allocation.

*Notations:* Bold-faced upper case letters, bold-faced lower case letters, and light-faced lower case letters denote matrices, column vectors, and scalar quantities, respectively. Superscripts  $(\cdot)^T$ ,  $(\cdot)^*$ , and  $(\cdot)^H$  represent transpose, conjugate, and conjugate-transpose operations, respectively.  $\mathcal{L}(\cdot)$  denotes the length of a vector.  $\Re\{\cdot\}$  and  $\Im\{\cdot\}$  denote the real and imaginary parts of a complex number.

## II. SYSTEM MODEL

Under BSs' non-cooperation scheme, we model a RIS-aided multi-user downlink communication system as in Fig.1. We assume that BS1 controls the RIS with  $M$  passive antennas, while the communication of BS2 should not be affected by the RIS. In detail, BS2 from another operator works under an orthogonal frequency band of BS1 and does not need the RIS. Let  $\boldsymbol{\theta} = [\theta_1, \theta_2, \dots, \theta_M]^H$  denote the RIS phase shift matrix and each element  $\theta_m, m = 1, \dots, M$  in  $\boldsymbol{\theta}$  could be expressed as  $\theta_m = \beta_m e^{j\alpha_m}$ . For maximum reflection efficiency, we let  $\beta_m = 1$  and  $\alpha_m \in [0, 2\pi]$ . The number of users served by BS1 and BS2 are  $K_s$  and  $K_i$ , respectively. All users are with a single antenna. Besides, both BS1 and BS2 have  $N$  elements. Specifically, we assume that the transmit beamforming vector at BS1 for a specific user  $k_s$  is  $\mathbf{w}_{k_s} \in \mathbb{C}^{N \times 1}$ .

We denote  $\mathbf{h}_{d_s} \in \mathbb{C}^{N \times 1}$ ,  $\mathbf{G}_s \in \mathbb{C}^{M \times N}$ , and  $\mathbf{h}_{r_s} \in \mathbb{C}^{M \times 1}$  as the channel expressions of BS1-user  $k_s$ , BS1-RIS, and RIS-user  $k_s$ , respectively, where  $k_s \in K_s$ . In addition, the power allocation vector of BS1 is denoted as  $\mathbf{p} \in \mathbb{C}^{1 \times K_s}$ . And  $\sum_{u=1}^{K_s} p_u \leq P_{\max}$  satisfies. Then the received signal at user  $k_s$  could be expressed as

$$y_{k_s} = (\mathbf{h}_{d_s}^H + \mathbf{h}_{r_s}^H \boldsymbol{\Theta} \mathbf{G}_s) \sum_{u=1}^{K_l} \mathbf{w}_u s_u p_u + n_{k_s}, \forall k_s \in K_s, \quad (1)$$

where  $\boldsymbol{\Theta} = \text{diag}(\boldsymbol{\theta}^T) \in \mathbb{C}^{M \times M}$  and  $n_{k_s}$  is the additive white Gaussian noise (AWGN) with zero mean and variance  $\sigma_n^2$ , i.e.,  $n_{k_s} \sim \mathcal{CN}(0, \sigma_n^2)$ . Assume that there are  $L$  sub-channels in total,  $K_l$  represents the number of users within the same  $l$ -th sub-channel of the user  $k_s$ , where  $K_l \leq K_{th}, \forall l \in L$ .  $K_{th}$  denotes the maximum number of users that one sub-channel can carry. We use matrix  $\mathbf{B} \in \mathbb{C}^{K_s \times L}$  to quantify the sub-channel assignment. Specifically,  $\mathbf{B}(k_s, l) = 1$  denotes that the user  $k_s$  is allocated to the  $l$ -th sub-channel; otherwise  $\mathbf{B}(k_s, l) = 0$ . Assume that each user can only be allocated to one sub-channel, then we have

$$\sum_{l=1}^L \mathbf{B}(k_s, l) = 1, \forall k_s \in K_s. \quad (2)$$

We apply the uniform linear array (ULA) configuration to channel vectors, which is generally expressed as

$$\mathbf{a}_{\text{ULA}}(\Omega, f) = [1, e^{j\frac{2\pi f}{c}d \cos \Omega}, \dots, e^{j\frac{2\pi f}{c}d(N_s-1) \cos \Omega}]^T. \quad (3)$$

We assume that the direct link  $\mathbf{h}_{d_s}$  follows Rayleigh fading, while RIS-aided channels  $\mathbf{h}_{r_s}$  and  $\mathbf{G}_s$  follow Rician fading. Then  $\mathbf{h}_{d_s}$ ,  $\mathbf{h}_{r_s}$ , and  $\mathbf{G}_s$  are modeled as

$$\mathbf{h}_{d_s} = \text{PL}_{\text{NLOS}} \bar{\mathbf{h}}_{d_s}, \quad (4)$$

$$\mathbf{h}_{r_s} = \text{PL}_{\text{LOS}, k_s} \left( \sqrt{\frac{\varepsilon}{\varepsilon + 1}} \mathbf{a}(\Omega_{R, k_s}, f_l) + \sqrt{\frac{1}{\varepsilon + 1}} \bar{\mathbf{h}}_{r_s} \right), \quad (5)$$

$$\mathbf{G}_s = \text{PL}_{\text{LOS}, 0} \left( \sqrt{\frac{\varepsilon}{\varepsilon + 1}} \mathbf{a}(\Omega_{R, 0}, f_l) \mathbf{a}^T(\Omega_B, f_l) + \sqrt{\frac{1}{\varepsilon + 1}} \bar{\mathbf{G}} \right). \quad (6)$$

Note that  $f_l$  denotes the operating frequency on the  $l$ -th sub-channel.  $\text{PL}_{\text{NLOS}}$ ,  $\text{PL}_{\text{LOS}, k_s}$  and  $\text{PL}_{\text{LOS}, 0}$  denote the corresponding path-loss.  $\varepsilon$  is the Rician factor.  $\Omega_{R, k_s}$ ,  $\Omega_{R, 0}$ , and  $\Omega_B$  denote the departing angle towards user  $k_s$ , incident angle at RIS and departing angle at BS towards RIS, respectively.  $\bar{\mathbf{h}}_{d_s}$ ,  $\bar{\mathbf{h}}_{r_s}$ , and  $\bar{\mathbf{G}}$  denote the NLOS components of channels, each element of which follows  $\mathcal{CN}(0, 1)$ .

Consider BS applying maximum ratio combining (MRC) for maximal power transmission, we approximate

$$\mathbf{w}_{k_s} = \mathbf{a}^*(\Omega_B, f_l), \forall k_s \in K_s. \quad (7)$$

For simplicity, we let  $\mathbf{w} = \mathbf{w}_{k_s}, \forall k_s \in K_s$ . Then we denote

$$\mathbf{h}_{d_s} = \mathbf{h}_{d_s}^H \mathbf{w}, \quad (8)$$

$$\mathbf{f}(\Omega_{R, 0}, f_l) = \mathbf{G}_s \mathbf{w}. \quad (9)$$

The received signal  $y_{k_s}$  in (1) can be transformed to

$$y_{k_s} = (\mathbf{h}_{d_s} + \mathbf{h}_{r_s}^H \boldsymbol{\Theta} \mathbf{f}(\Omega_{R, 0}, f_l)) \sum_{u=1}^{K_l} s_u p_u + n_{k_s}. \quad (10)$$

We abbreviate  $\mathbf{f}(\Omega_{R, 0}, f_l)$  to  $\mathbf{f}$  throughout the paper. Then, the SNR for the user  $k_s$  could be represented as

$$\text{SNR}_{k_s} = \frac{|(\mathbf{h}_{d_s} + \mathbf{h}_{r_s}^H \boldsymbol{\Theta} \mathbf{f})|^2 p_{k_s}}{|(\mathbf{h}_{d_s} + \mathbf{h}_{r_s}^H \boldsymbol{\Theta} \mathbf{f})|^2 \sum_{u \neq k_s}^{K_l} p_u + \sigma_n^2}, \quad (11)$$

where  $\text{SNR}_{k_s} \geq \text{SNR}_{th}, \forall k_s \in K_s$ . Based on (11), we could get the expression of the sum-rate of users served by BS1 as

$$R = \sum_{u=1}^{K_s} \log_2(1 + \text{SNR}_u). \quad (12)$$

In addition, the BS2-user  $k_i$ , BS2-RIS, and RIS-user  $k_i$  links are defined as  $\mathbf{h}_{d_i} \in \mathbb{C}^{N \times 1}$ ,  $\mathbf{G}_i \in \mathbb{C}^{M \times N}$ , and

$\mathbf{h}_{r_i} \in \mathbb{C}^{M \times 1}$ . The signal received by the user  $k_i$  within the adjacent cell and served by BS2 could be expressed as

$$y_{k_i} = (\mathbf{h}_{d_i}^H + \mathbf{h}_{r_i}^H \Theta \mathbf{G}_i) \sum_{r=1}^{K_i} \mathbf{w}_r s_r p_r + n_{k_i}, \forall k_i \in K_i. \quad (13)$$

Consider the non-cooperation scheme, i.e., to mitigate the effect of RIS on BS2-user  $k_i$  links, the user  $k_i, \forall k_i \in K_i$  would receive comparable signals when only direct link exists as when the RIS-aided reflective links also exist. Then we have

$$y_{k_i} \approx \mathbf{h}_{d_i}^H \sum_{r=1}^{K_i} \mathbf{w}_r s_r p_r + n_{k_i}. \quad (14)$$

By combining (13) and (14), we get

$$\|\mathbf{h}_{r_i}^H \Theta \mathbf{G}_i\| \leq \delta, \quad \forall k_i \in K_i, \quad (15)$$

where  $\delta$  denotes the threshold for the channel gain of the reflective link BS2-RIS-user  $k_i$ , which should satisfy  $0 < \delta \ll 1$  to guarantee the largely mitigated impact of RIS.

By jointly considering the power allocation  $\mathbf{p}$ , sub-channel assignment  $\mathbf{B}$  at BS1, and the RIS passive beamforming  $\theta$ , we formulate the following optimization problem:

$$\mathbb{P} : \max_{\mathbf{p}, \mathbf{B}, \theta} R \quad (16a)$$

$$\text{s.t.} \quad \text{SNR}_{k_s} \geq \text{SNR}_{th}, \forall k_s \in K_s, \quad (16b)$$

$$\|\mathbf{h}_{r_i}^H \Theta \mathbf{G}_i\| \leq \delta, \forall k_i \in K_i, \quad (16c)$$

$$K_l \leq K_{th}, \forall l \in L, \quad (16d)$$

$$\sum_{u=1}^{K_s} p_u \leq P_{\max}, \quad (16e)$$

$$\sum_{l=1}^L \mathbf{B}(k_s, l) = 1, \forall k_s \in K_s, \quad (16f)$$

$$|\theta_m| = 1, m = 1, \dots, M. \quad (16g)$$

Note that this problem is challenging due to the non-convexity of the objective function and multiple constraints. And there is no standard method to get a global-optimal solution. In the following, we develop the block coordinate descent (BCD) algorithm to solve the problem  $\mathbb{P}$ .

### III. THE PROPOSED ALGORITHM FOR SUM-RATE MAXIMIZATION

To solve the formulated optimization problem above, we first tackle the discrete sub-channel assignment optimization of  $\mathbf{B}$ . Then we optimize  $\mathbf{p}$  and  $\theta$  sequentially while keeping another variable fixed. Our optimization can be therefore divided into the following three sub-problems.

#### A. Optimization of sub-channel assignment $\mathbf{B}$

We firstly initialize  $\mathbf{p}$  as  $p_{k_s} = P_{\max}/K_s, \forall k_s \in K_s$ . And  $\theta$  is initialized as  $\theta_m = \angle \mathbf{h}_{d_s} - \angle [\mathbf{g}_s]_m$  as in [7], where  $\mathbf{g}_s = \mathbf{h}_{r-s}^H \text{diag}(\mathbf{f})$ , and  $[\mathbf{h}_{d_s}, \mathbf{g}_s] = \arg \min_{k_s \in K_s} |h_{d_s}|$ . With fixed  $\mathbf{p}$  and  $\theta$ , the formulated problem can be transformed as

$$\mathbb{P}1 : \max_{\mathbf{B}} R \quad (17)$$

$$\text{s.t.} \quad (16b), (16d), (16f). \quad (18)$$

---

#### Algorithm 1 Sub-channel assignment optimization based on TSM algorithm — Matching Sets Initialization

---

**Input:**  $\mathbf{Z} = \mathbf{0} \in \mathbb{C}^{K_s \times L}, \mathbf{r} = [ ]$ ,  $\mathcal{K} = \{1, \dots, K_s\}$ ,  $\mathbf{s}_0 = \mathbf{0} \in \mathbb{C}^{1 \times K_s}, \mathbf{v} = \mathbf{0} \in \mathbb{C}^{1 \times K_s}$ .

**while**  $\mathcal{K} \neq \{ \}$  **do**

2:   **for**  $i = 1 : \mathcal{L}(\mathcal{K})$  **do**

**for**  $l = 1 : L$  **do**

**if**  $\mathbf{Z}(\mathcal{K}(i), l) == 0$  **then**

$\mathbf{g}(l) = |(h_{d_s} + \mathbf{h}_{r-s}^H \Theta \mathbf{f})|^2$ ;

**else**

$\mathbf{g}(l) = 0$ ;

**end if**

**end for**

$[\mathbf{v}(\mathcal{K}(i)), \mathbf{s}_0(\mathcal{K}(i))] = \max(\mathbf{g})$ ;

**end for**

12:   **for**  $l = 1 : L$  **do**

$\mathbf{x} = \text{find}(\mathbf{s}_0 == l)$ ;

14:       **if**  $\mathcal{L}(\mathbf{x}) \leq K_{th}$  **then**

$\mathbf{Z}(\mathbf{x}, l) = 1$ ;

16:       **else**

          get  $\tilde{\mathbf{x}}$  as the sorted  $\mathbf{x}$  corresponding to  $\mathbf{v}(\tilde{\mathbf{x}})$  in a descend manner;

18:       update  $\mathbf{Z}(\tilde{\mathbf{x}}(1 : K_s), l) = 1$ , and  $\mathbf{Z}(\tilde{\mathbf{x}}(K_s + 1 : \mathcal{L}(\mathbf{x})), l) = 2$ ;

**end if**

20:       **end for**

$[\mathbf{r}, \mathbf{c}] = \text{find}(\mathbf{Z} == 1)$ ,  $\mathcal{K} = \mathcal{K} \setminus \mathbf{r}$ ;

22:   **end while**

**Output:**  $\mathbf{s}_0$ .

---

In order to solve this discrete optimization problem, the two-sided matching (TSM) algorithm [10] is applied. Specifically, the algorithm can be decomposed into two processes.

- **Matching sets initialization:** We firstly initialize  $\mathbf{Z} = \mathbf{0} \in \mathbb{C}^{K_s \times L}$ , which records the matching states between users and sub-channels. Specifically, '0', '1', and '2' denote 'Unallocated', 'Accepted', and 'Rejected', respectively. In each iteration, we calculate the channel gain  $|(h_{d_s} + \mathbf{h}_{r-s}^H \Theta \mathbf{f})|^2$  for all users that have not been accepted. The channel gains vary on different sub-channels. Then users are assigned to channels that can achieve the highest gains and have not been rejected by that channel before. After that, the sub-channel chooses users with highest channel gain and rejects the others. The iteration ends when all users are accepted by one specific sub-channel. The procedure is shown as **Algorithm 1**.
- **Matching stability verification:** An unstable matching pair is defined as a pair of elements that prefer each other over the state they have already matched. A user will be paired with others that are allocated to different sub-channels in each iteration. Assume that the user is on the  $l$ -th sub-channel and the potential switching user is on the  $\tilde{l}$ -th sub-channel. The sum-rate on the  $l$ -th sub-channel before and after switching is defined as  $R_1$  and  $\tilde{R}_1$ , respectively. Similarly, the sum-rate on the  $\tilde{l}$ -th sub-channel before and after switching is  $R_2$  and  $\tilde{R}_2$ ,

---

**Algorithm 2** Sub-channel assignment optimization based on TSM algorithm — Matching Stability Verification

---

**Input:**  $s_0$ .

**for**  $i = 1 : K_s$  **do**

2:  $\mathbf{b} = \mathbf{0} \in \mathbb{C}^{1 \times K_s}$ ;

$\mathbf{f} = \text{find}(s_0 == s_0(i))$ ;

4: Find the set of users allocated to different sub-channels to the  $i$ -th user by  $\mathbf{d} = \{1, \dots, K_s\} \setminus \mathbf{f}$ ;

**for**  $j = 1 : \mathcal{L}(\mathbf{d})$  **do**

6:  $\tilde{l} = s_0(j)$ ;

calculate  $R_1$  and  $R_2$ ;

8: swap the  $i$ -th and  $\tilde{d}(j)$ -th user to each other's sub-channel; calculate  $\tilde{R}_1$  and  $\tilde{R}_2$ ;

**if**  $|\tilde{R}_1 + \tilde{R}_2| \geq |R_1 + R_2|$  &&  $\text{SNR}_u \geq \text{SNR}_{th}$ ,  $\text{SNR}_u \in \{\text{SNR}_l, \text{SNR}_{\tilde{l}}\}$  **then**

10:  $\mathbf{b}(\tilde{d}(j)) = |\tilde{R}_1 + \tilde{R}_2 - R_1 - R_2|$ ;

**end if**

12: Find the maximum value in  $\mathbf{b}$  and the corresponding  $\tilde{d}(j)$ -th user;

$s_0(i) \leftrightarrow s_0(\tilde{d}(j))$ ;

14: update  $\hat{s}_0 = s_0$ ;

**end for**

16: **end for**

**Output:**  $\hat{s}_0$ .

---

respectively. Then the switching pair is determined by (a)  $\max|\tilde{R}_1 + \tilde{R}_2 - R_1 - R_2|$ ; (b)  $\text{SNR}_u \geq \text{SNR}_{th}$ ,  $\text{SNR}_u \in \{\text{SNR}_l, \text{SNR}_{\tilde{l}}\}$ , where  $\{\text{SNR}_l, \text{SNR}_{\tilde{l}}\}$  denotes the SNR sets of users on  $l$ -th and  $\tilde{l}$ -th sub-channels. This procedure is summarized as in **Algorithm 2**.

The output  $\hat{s}_0$  can be easily transformed to the optimized matrix  $\mathbf{B}_{\text{opt}} \in \mathbb{C}^{K_s \times L}$  by  $\mathbf{B}_{\text{opt}}(k_s, \hat{s}_0(k_s)) = 1, \forall k_s \in K_s$ , while other elements in  $\mathbf{B}_{\text{opt}}$  are fixed to be 0.

### B. Optimization of power allocation $\mathbf{p}$

Given  $\mathbf{B}$  and  $\boldsymbol{\theta}$ , the problem  $\mathbb{P}$  can be simplified as

$$\mathbb{P}2: \max_{\mathbf{p}} R \quad (19)$$

$$\text{s.t.} \quad (16b), (16e). \quad (20)$$

To address the non-convexity of the objective function, we introduce a new variable set  $\boldsymbol{\chi} = \{\chi_1, \dots, \chi_{K_s}\}$ . Then we let

$$\frac{|(h_{d_s} + \mathbf{h}_{r_s}^H \boldsymbol{\Theta} \mathbf{f})|^2 p_{k_s}}{|(h_{d_s} + \mathbf{h}_{r_s}^H \boldsymbol{\Theta} \mathbf{f})|^2 \sum_{u \neq k_s}^{K_l} p_u + \sigma_n^2} \geq \chi_{k_s}, \forall k_s \in K_s, \quad (21)$$

which could be further represented as

$$p_{k_s} \geq \chi_{k_s} \left( \sum_{u \neq k_s}^{K_l} p_u + \mu_{k_s} \right), \forall k_s \in K_s, \quad (22)$$

where  $\mu_{k_s} = \frac{\sigma_n^2}{|(h_{d_s} + \mathbf{h}_{r_s}^H \boldsymbol{\Theta} \mathbf{f})|^2}$ . The optimization problem  $\mathbb{P}2$  can be then rewritten as

$$\mathbb{P}2.1: \max_{\mathbf{p}, \boldsymbol{\chi}} \sum_{u=1}^{K_s} \log_2(1 + \chi_u) \quad (23)$$

$$\text{s.t.} \quad \chi_{k_s} \geq \text{SNR}_{th}, \forall k_s \in K_s \quad (24)$$

$$(16e), (22). \quad (25)$$

---

**Algorithm 3** Proposed power allocation algorithm based on convex upper bound approximation

---

**Input:**  $\mathbf{p}^0 \in \mathbb{C}^{1 \times K_s}$ ,  $\boldsymbol{\chi}^0 \in \mathbb{C}^{1 \times K_s}$ ,  $t_1 = 1$ .

**repeat**

2: Obtain  $\alpha_{k_s}^{t_1}, \forall k_s \in K_s$  by (27);

Solve  $\mathbb{P}2.2$  by CVX toolbox, and get  $\mathbf{p}^{t_1}, \boldsymbol{\chi}^{t_1}$ ;

4:  $t_1 = t_1 + 1$ ;

**until** convergence reaches

**Output:**  $\mathbf{p}^{t_1}, \boldsymbol{\chi}^{t_1}$ .

---



---

**Algorithm 4** Proposed RIS beamforming optimization based on SCA

---

**Input:**  $\boldsymbol{\theta}^0 \in \mathbb{C}^{M \times 1}$ ,  $t_2 = 1$ .

**repeat**

2: Obtain  $\zeta_{k_s}^{t_2-1}$  and  $t_{k_s}^{t_2-1}$  by (46) and (47);

Obtain  $\boldsymbol{\lambda}^{t_2} \in \mathbb{C}^{K_s \times 1}$  by (34);

4: Solve  $\mathbb{P}3.3$  by CVX toolbox, and get  $\boldsymbol{\theta}^{t_2}$ ;

$t_2 = t_2 + 1$ ;

6: **until** convergence reaches

**Output:**  $\boldsymbol{\theta}^{t_2}$ .

---

However, (22) is still non-convex. In order to address this issue, we apply the convex upper bound approximation [11].

**Lemma 1:** Given  $g(x, y) = xy$  and  $f(x, y) = \frac{\alpha}{2}x^2 + \frac{1}{2\alpha}y^2$  ( $\alpha > 0$ ),  $f(x, y) \geq g(x, y)$  always holds. Specifically, when  $\alpha = \frac{y}{x}$ , there are  $f(x, y) = g(x, y)$ . Note that  $f(x, y)$  is convex.

Based on **Lemma 1**, we rewrite the non-convex term  $\chi_{k_s} \sum_{u \neq k_s}^{K_l} p_u$  in (22) as

$$\chi_{k_s} \sum_{u \neq k_s}^{K_l} p_u \leq \frac{\alpha_{k_s}}{2} \chi_{k_s}^2 + \frac{1}{2\alpha_{k_s}} \left( \sum_{u \neq k_s}^{K_l} p_u \right)^2. \quad (26)$$

When  $\alpha_{k_s} = \frac{\sum_{u \neq k_s}^{K_l} p_u}{\chi_{k_s}}$ , the equality holds. Then successive convex approximation algorithm is applied to solve  $\mathbb{P}2$ . Specifically, the  $\alpha_{k_s}^{t_1}$  in the  $t_1$ -th iteration is obtained by  $(\sum_{u \neq k_s}^{K_l} p_u)^{t_1-1}$  and  $\chi_{k_s}^{t_1-1}$ , which is expressed as

$$\alpha_{k_s}^{t_1} = \frac{(\sum_{u \neq k_s}^{K_l} p_u)^{t_1-1}}{\chi_{k_s}^{t_1-1}}. \quad (27)$$

And (22) can be consequently rewritten in the convex form as

$$p_{k_s} \geq \frac{\alpha_{k_s}^{t_1}}{2} \chi_{k_s}^2 + \frac{1}{2\alpha_{k_s}^{t_1}} \left( \sum_{u \neq k_s}^{K_l} p_u \right)^2 + \chi_{k_s} \mu_{k_s}, \forall k_s \in K_s. \quad (28)$$

The optimization of  $\mathbb{P}2$  can be therefore transformed into iteratively solving the problem  $\mathbb{P}2.2$ , which is expressed as

$$\mathbb{P}2.2 \max_{\mathbf{p}, \boldsymbol{\chi}} \sum_{u=1}^{K_s} \log_2(1 + \chi_u) \quad (29)$$

$$\text{s.t.} \quad (16e), (24), (28). \quad (30)$$

Note that the problem  $\mathbb{P}2.2$  is convex and can be easily solved by CVX toolbox. The iteration ends until it converges. The algorithm is summarized as **Algorithm 3**. Finally, we get the optimized power allocation vector  $\hat{\mathbf{p}} = \mathbf{p}^{t_1}$ .

### C. Optimization of RIS passive beamforming $\boldsymbol{\theta}$

We fix the variables  $\mathbf{p}$  and  $\mathbf{B}$  and optimize  $\boldsymbol{\theta}$ , then the problem  $\mathbb{P}$  can be simplified as

$$\mathbb{P}3 \quad \max_{\boldsymbol{\theta}} \quad \mathcal{O}(\boldsymbol{\theta}) = R \quad (31)$$

$$\text{s.t.} \quad (16\text{b}), (16\text{c}), (16\text{g}). \quad (32)$$

Inspired by [12], the objective function in  $\mathbb{P}3$  is a standard multi-ratio fractional programming (FP) problem. The quadratic transformation method is applied, which efficiently transforms the fractional form into a quadratic function. Specifically, we introduce a new variable set  $\boldsymbol{\lambda} = [\lambda_1, \dots, \lambda_{K_s}]^T$ , and we further define  $\mathbf{g}_s = \text{diag}(\mathbf{h}_{r_s}^H) \mathbf{f}$ . Then the objective function is rewritten as

$$\begin{aligned} \mathcal{O}(\boldsymbol{\lambda}, \boldsymbol{\theta}) = & \sum_{k_s \in K_s} \log_2(1 + 2\lambda_{k_s} \sqrt{p_{k_s}} \text{Re}\{h_{d_s} + \boldsymbol{\theta}^H \mathbf{g}_s\}) \\ & - \lambda_{k_s}^2 \left( \sum_{u \neq k_s}^{K_l} p_u |h_{d_s} + \boldsymbol{\theta}^H \mathbf{g}_s|^2 + \sigma_n^2 \right), \end{aligned} \quad (33)$$

which can be maximized by iteratively optimizing  $\boldsymbol{\lambda}$  and  $\boldsymbol{\theta}$ . Particularly, with the optimized  $\boldsymbol{\theta}^{t_2-1}$  in the  $(t_2 - 1)$ -th iteration, the  $\lambda_{k_s}^{t_2}$  can be obtained as

$$\lambda_{k_s}^{t_2} = \frac{\sqrt{p_{k_s}} \text{Re}\{h_{d_s} + (\boldsymbol{\theta}^{t_2-1})^H \mathbf{g}_s\}}{\ln(2) \left( \sum_{u \neq k_s}^{K_l} p_u |h_{d_s} + (\boldsymbol{\theta}^{t_2-1})^H \mathbf{g}_s|^2 + \sigma_n^2 \right)}. \quad (34)$$

With given  $\lambda_{k_s}^{t_2}$ , the  $\text{SNR}_{k_s}$  with respect to  $\boldsymbol{\theta}$  is denoted as

$$\text{SNR}_{k_s} = -\boldsymbol{\theta}^H \boldsymbol{\Lambda}_{k_s} \boldsymbol{\theta} + 2\text{Re}\{\boldsymbol{\theta}^H \mathbf{v}_{k_s}\} + \varphi_{k_s}, \quad (35)$$

where  $\boldsymbol{\Lambda}_{k_s}, \mathbf{v}_{k_s}$ , and  $\varphi_{k_s}$  are defined as

$$\boldsymbol{\Lambda}_{k_s} = (\lambda_{k_s}^{t_2})^2 \sum_{u \neq k_s}^{K_l} p_u (h_{d_s} + \mathbf{g}_s \mathbf{g}_s^H), \quad (36)$$

$$\mathbf{v}_{k_s} = 2\lambda_{k_s}^{t_2} \sqrt{p_{k_s}} \mathbf{g}_s - (\lambda_{k_s}^{t_2})^2 \sum_{u \neq k_s}^{K_l} p_u h_{d_s}^* \mathbf{g}_s, \quad (37)$$

$$\varphi_{k_s} = 2\lambda_{k_s}^{t_2} \sqrt{p_{k_s}} \text{Re}\{h_{d_s}\} - (\lambda_{k_s}^{t_2})^2 \left( \sum_{u \neq k_s}^{K_l} p_u |h_{d_s}|^2 + \sigma_n^2 \right). \quad (38)$$

Then by taking (35) into the objective function, the optimization of  $\boldsymbol{\theta}$  in the  $t_2$ -th iteration could be summarized as

$$\mathbb{P}3.1 \quad \max_{\boldsymbol{\theta}} \quad \sum_{u=1}^{K_s} \log_2(1 + \text{SNR}_u) \quad (39)$$

$$\text{s.t.} \quad (16\text{b}), (16\text{c}), (16\text{g}). \quad (40)$$

We notice that  $\mathbb{P}3.1$  is still non-convex due to the non-convex constraint (16b) and (16g). To address the non-convexity of (16g), the penalty method is firstly applied, which rewrite (16g) into the objective function by multiplying a positive penalty factor  $\tau$ . Then the objective function could be concisely expressed as

$$\mathcal{O}'(\boldsymbol{\theta}) = \sum_{u=1}^{K_s} \log_2(1 + \text{SNR}_u) + \tau \sum_{m=1}^M (|\theta_m|^2 - 1). \quad (41)$$

Sequentially,  $\mathbb{P}3.1$  can be rewritten as

$$\mathbb{P}3.2 \quad \max_{\boldsymbol{\theta}} \quad \mathcal{O}'(\boldsymbol{\theta}) \quad (42)$$

$$\text{s.t.} \quad (16\text{b}), (16\text{c}) \quad (43)$$

$$|\theta_m| \leq 1, \quad m = 1, \dots, M. \quad (44)$$

---

**Algorithm 5** The overall BCD algorithm

---

**Input:**  $\boldsymbol{\theta}^0 \in \mathbb{C}^{M \times 1}$ ,  $\mathbf{p}^0 \in \mathbb{C}^{M \times 1}$ ,  $t = 1$ .

Obtain  $\mathbf{s}_0$  by **Algorithm 1**;

2: Obtain  $\hat{\mathbf{s}}_0$  by **Algorithm 2**;

Obtain  $\mathbf{B}_{\text{opt}} \in \mathbb{C}^{K_s \times L}$  based on  $\hat{\mathbf{s}}_0$ .

4: **repeat**

Given  $\mathbf{B}_{\text{opt}}$  and  $\boldsymbol{\theta}^{t-1}$ , obtain  $\mathbf{p}^t$  by **Algorithm 3**;

6: Given  $\mathbf{B}_{\text{opt}}$  and  $\mathbf{p}^t$ , obtain  $\boldsymbol{\theta}^t$  by **Algorithm 4**;

$t = t + 1$ ;

8: **until** convergence reaches

$\mathbf{p}_{\text{opt}} = \mathbf{p}^t$ , and  $\boldsymbol{\theta}_{\text{opt}} = \boldsymbol{\theta}^t$ ;

**Output:**  $\mathbf{B}_{\text{opt}}$ ,  $\mathbf{p}_{\text{opt}}$ , and  $\boldsymbol{\theta}_{\text{opt}}$ .

---

Then, we deal with the non-convexity of the non-convex term in  $\mathcal{O}'(\boldsymbol{\theta})$  and (16b) by successive cancellation algorithm (SCA). We represent the first-order Taylor series approximation of the objective function as

$$\mathcal{O}''(\boldsymbol{\theta}) = \sum_{u=1}^{K_s} \log_2(1 + \text{SNR}_u) + \tau \sum_{m=1}^M \theta_m^{t_2} (\theta_m - \theta_m^{t_2}). \quad (45)$$

We further define

$$\tau_{k_s} = \text{Re}\{h_{d_s} + \boldsymbol{\theta}^H \mathbf{g}_s\}, \quad (46)$$

$$i_{k_s} = \text{Im}\{h_{d_s} + \boldsymbol{\theta}^H \mathbf{g}_s\}. \quad (47)$$

Similarly, by applying the first-order Taylor series expansion, (16b) can be rewritten as

$$\begin{aligned} & (\tau_{k_s}^{t_2-1})^2 + (i_{k_s}^{t_2-1})^2 + 2\tau_{k_s}^{t_2-1} (\tau_{k_s} - \tau_{k_s}^{t_2-1}) + \\ & 2i_{k_s}^{t_2-1} (i_{k_s} - i_{k_s}^{t_2-1}) \geq (\tau_{k_s}^2 + i_{k_s}^2) \epsilon + \xi, \forall k_s \in K_s, \end{aligned} \quad (48)$$

where

$$\epsilon = \frac{\text{SNR}_{th} \sum_{u \neq k_s}^{K_l} p_u}{p_{k_s}}, \quad (49)$$

$$\xi = \frac{\text{SNR}_{th} \sigma_n^2}{p_{k_s}}. \quad (50)$$

Finally, the corresponding convex optimization problem with respect to  $\boldsymbol{\theta}$  can be formulated as

$$\mathbb{P}3.3 \quad \max_{\boldsymbol{\theta}} \quad \mathcal{O}''(\boldsymbol{\theta}) \quad (51)$$

$$\text{s.t.} \quad (16\text{c}), (44), (48). \quad (52)$$

The SCA is used to iteratively optimize  $\boldsymbol{\theta}$ , while in each iteration, the problem  $\mathbb{P}3.3$  is a standard convex optimization problem and can be solved by CVX toolbox. The algorithm is summarized as **Algorithm 4**.

*D. The overall BCD algorithm*

The overall algorithm for sum-rate maximization via jointly optimizing sub-channel assignment  $\mathbf{B}$ , power allocation  $\mathbf{p}$ , and passive RIS beamforming  $\boldsymbol{\theta}$  is summarized as **Algorithm 5**.

## IV. SIMULATION RESULTS

In this section, numerical examples are demonstrated to verify the effectiveness of our system model and algorithms. We place BS1, BS2, and RIS at (200m, 30m), (220m, 30m), and (200m, 0), respectively. The radius of both cells is set to be 10m. Assume that there are 20 SUs and 20 IUs. The center frequency of BS1's working band is 2.5 GHz. The frequency band is divided into  $L = 10$  sub-channels, where

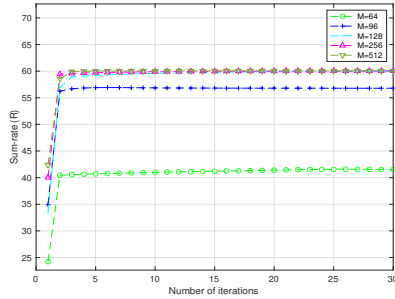


Fig. 2. Convergence behaviour of the proposed algorithm.

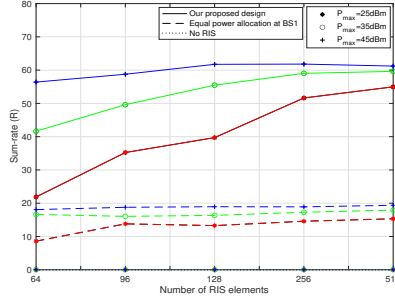


Fig. 3. The Sum-rate for  $M = \{64, 96, 128, 256, 512\}$ , and  $P_{\max} = \{25, 35, 45\}$  dBm.

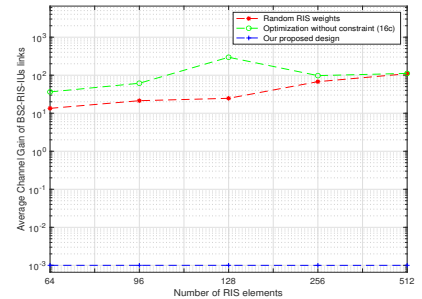


Fig. 4. The effects of RIS on BS2-RIS-IUs links under different number of RIS elements.

the bandwidth of each sub-channel is 20 kHz and can tolerate up to 2 users, i.e.,  $K_{th} = 2$ . The Rician factor of RIS-aided channels is set to be 10. The path-loss in dB as a function of distance  $d$  is defined as  $PL_{LOS} = 112.6 + 22.0 \log(d)$  and  $PL_{NLOS} = 109.6 + 36.7 \log(d)$  for LOS and NLOS paths, respectively. The SNR constraint for SUs is set as  $SNR_{th} = 0.01$ , and the constraint for the channel gain of BS2-RIS-IUs is set as  $\delta = 0.001$ .

Fig. 2 demonstrates the convergence of our proposed algorithm. The transmit power at BS1 is set as  $P_{\max} = 35$  dBm. And we verify the convergence under different RIS elements. It can be seen that the sum-rate of users served by BS1 increases rapidly at initial, and converges to a stable value within limited iterations.

In Fig. 3, we study the effects of RIS reflecting elements and the total transmit power. Our proposed design is compared with the cases that (a) equal power allocation at BS1; (b) no RIS is deployed. And we relax the SNR constraint (16b) under no RIS case as it can not be realized without the RIS-aided channels. Fig. 3 depicts that when only direct links exist, the sum-rate could be extremely low. By introducing RIS and proposing passive beamforming design, the sum-rate increases significantly. Compared with the RIS-aided system where the transmit power is equally allocated, the achievable sum-rate can be further improved by optimizing the power allocation.

Fig. 4 investigates the effects of RIS on BS2 - IUs channels. The random RIS weights design and optimization without constraint on the BS2-RIS-IUs links, i.e., (16c), are used for comparison. It can be seen that both designs for comparison result in high average channel gains of BS2-RIS-IUs links, revealing severe effects taken by RIS to the quality-of-service (QoS) in the cell worked by BS2. In contrast, our proposed design enables low average channel gain of the reflective links, satisfying  $\|\mathbf{h}_{r-i}^H \Theta \mathbf{G}_i\| \leq \delta, \forall k_i \in K_i$ . It can be concluded that our proposed design alleviates the impacts of RIS on BS2-served cell to large extents.

## V. CONCLUSION

In this paper, we propose RIS-aided resource allocation under BSs' non-cooperation scheme. The study of non-cooperation scheme in RIS-aided systems is crucial since BSs may not jointly use the same RIS. Specifically, we consider that the RIS is solely controlled by one BS and cannot affect

the communication of others. For users served by the RIS-aided BS, the sum-rate is maximized by jointly optimizing sub-channel assignment, power allocation, and passive RIS beamforming. On a parallel avenue, the RIS is designed to alleviate its effect on the links between the adjacent BS and its serving users. A BCD algorithm is applied to solve the non-convex optimization problem.

## REFERENCES

- [1] C. Liaskos, S. Nie, A. Tsioliaridou, A. Pitsillides, S. Ioannidis, and I. Akyildiz, "A New Wireless Communication Paradigm through Software-Controlled Metasurfaces," *IEEE Communications Magazine*, vol. 56, no. 9, pp. 162–169, 2018.
- [2] J. Rains, J. ur Rehman Kazim, A. Tukmanov, L. Zhang, Q. H. Abbasi, and M. A. Imran, *Practical Design Considerations for Reconfigurable Intelligent Surfaces*, 2023, pp. 99–122.
- [3] H. Ren, X. Liu, C. Pan, Z. Peng, and J. Wang, "Performance Analysis for RIS-Aided Secure Massive MIMO Systems With Statistical CSI," *IEEE Wireless Communications Letters*, vol. 12, no. 1, pp. 124–128, 2023.
- [4] H. Wang, C. Liu, Z. Shi, Y. Fu, and R. Song, "GSIC for RIS-Aided Uplink Multi-Antenna NOMA Systems," *IEEE Communications Letters*, vol. 26, no. 1, pp. 187–191, 2022.
- [5] Y. Liu, L. Zhang, F. Gao, and M. A. Imran, "Intelligent Reflecting Surface Networks With Multiorder-Reflection Effect: System Modeling and Critical Bounds," *IEEE Transactions on Communications*, vol. 70, no. 10, pp. 6992–7005, 2022.
- [6] L. Kong, S. Kisseleff, S. Chatzinotas, B. Ottersten, and M. Erol-Kantarci, "Effective Rate of RIS-aided Networks with Location and Phase Estimation Uncertainty," in *2022 IEEE Wireless Communications and Networking Conference (WCNC)*, 2022, pp. 2071–2075.
- [7] J. Zuo, Y. Liu, Z. Qin, and N. Al-Dhahir, "Resource Allocation in Intelligent Reflecting Surface Assisted NOMA Systems," *IEEE Transactions on Communications*, vol. 68, no. 11, pp. 7170–7183, 2020.
- [8] D. Zhao, H. Lu, Y. Wang, and H. Sun, "Joint Passive Beamforming and User Association Optimization for IRS-assisted mmWave Systems," in *GLOBECOM 2020 - 2020 IEEE Global Communications Conference*, 2020, pp. 1–6.
- [9] D. Zhao, H. Lu, Y. Wang, H. Sun, and Y. Gui, "Joint Power Allocation and User Association Optimization for IRS-Assisted mmWave Systems," *IEEE Transactions on Wireless Communications*, vol. 21, no. 1, pp. 577–590, 2022.
- [10] P. Gupta and D. Ghosh, "User Fairness based Energy Efficient Power Allocation for Downlink Cellular NOMA System," in *2020 5th International Conference on Computing, Communication and Security (ICCCS)*, 2020, pp. 1–5.
- [11] L.-N. Tran, M. F. Hanif, A. Tolli, and M. Juntti, "Fast Converging Algorithm for Weighted Sum Rate Maximization in Multicell MISO Downlink," *IEEE Signal Processing Letters*, vol. 19, no. 12, pp. 872–875, 2012.
- [12] K. Shen and W. Yu, "Fractional Programming for Communication Systems—Part I: Power Control and Beamforming," *IEEE Transactions on Signal Processing*, vol. 66, no. 10, pp. 2616–2630, 2018.